ESC European Society of Cardiology

Cardiovascular Research (2022) **118**, 1020–1032
doi:10.1093/cvr/cvab123

SERCA2a stimulation by istaroxime improves intracellular Ca^{2+} handling and diastolic dysfunction in a model of diabetic cardiomyopathy

Eleonora Torre [1], Martina Arici [1], Alessandra Maria Lodrini [1], Mara Ferrandi [2], Paolo Barassi[2], Shih-Che Hsu[3], Gwo-Jyh Chang [4], Elisabetta Boz[5], Emanuela Sala [1], Sara Vagni[1], Claudia Altomare [6], Gaspare Mostacciuolo[1], Claudio Bussadori [5], Patrizia Ferrari[2], Giuseppe Bianchi[2], and Marcella Rocchetti [1]*

[1]Department of Biotechnology and Biosciences, Università degli Studi di Milano-Bicocca, Milan, Italy; [2]Windtree Therapeutics Inc., Warrington, PA, USA; [3]CVie Therapeutics Limited, Taipei, Taiwan; [4]Graduate Institute of Clinical Medical Sciences, Chang Gung University, Tao-Yuan 33305, Taiwan; [5]Clinica Veterinaria Gran Sasso Via Donatello, 26, 20131 Milano, Italy; and [6]Fondazione Cardiocentro Ticino, via Tesserete 48, Lugano 6900, Switzerland

Received 12 November 2020; revised 20 January 2021; editorial decision 22 March 2021; accepted 31 March 2021; online publish-ahead-of-print 1 April 2021

Aims Diabetic cardiomyopathy is a multifactorial disease characterized by an early onset of diastolic dysfunction (DD) that precedes the development of systolic impairment. Mechanisms that can restore cardiac relaxation improving intracellular Ca^{2+} dynamics represent a promising therapeutic approach for cardiovascular diseases associated to DD. Istaroxime has the dual properties to accelerate Ca^{2+} uptake into sarcoplasmic reticulum (SR) through the SR Ca^{2+} pump (SERCA2a) stimulation and to inhibit Na^{+}/K^{+} ATPase (NKA). This project aims to characterize istaroxime effects at a concentration (100 nmol/L) marginally affecting NKA, in order to highlight its effects dependent on the stimulation of SERCA2a in an animal model of mild diabetes.

Methods and results Streptozotocin (STZ) treated diabetic rats were studied at 9 weeks after STZ injection in comparison to controls (CTR). Istaroxime effects were evaluated *in vivo* and in left ventricular (LV) preparations. STZ animals showed (i) marked DD not associated to cardiac fibrosis, (ii) LV mass reduction associated to reduced LV cell dimension and T-tubules loss, (iii) reduced LV SERCA2 protein level and activity and (iv) slower SR Ca^{2+} uptake rate, (v) LV action potential (AP) prolongation and increased short-term variability (STV) of AP duration, (vi) increased diastolic Ca^{2+}, and (vii) unaltered SR Ca^{2+} content and stability in intact cells. Acute istaroxime infusion (0.11 mg/kg/min for 15 min) reduced DD in STZ rats. Accordingly, in STZ myocytes istaroxime (100 nmol/L) stimulated SERCA2a activity and blunted STZ-induced abnormalities in LV Ca^{2+} dynamics. In CTR myocytes, istaroxime increased diastolic Ca^{2+} level due to NKA blockade albeit minimal, while its effects on SERCA2a were almost absent.

Conclusions SERCA2a stimulation by istaroxime improved STZ-induced DD and intracellular Ca^{2+} handling anomalies. Thus, SERCA2a stimulation can be considered a promising therapeutic approach for DD treatment.

*Corresponding author. Tel: +39 0264483313; fax: +39 0264483565, E-mail: marcella.rocchetti@unimib.it

Graphical Abstract

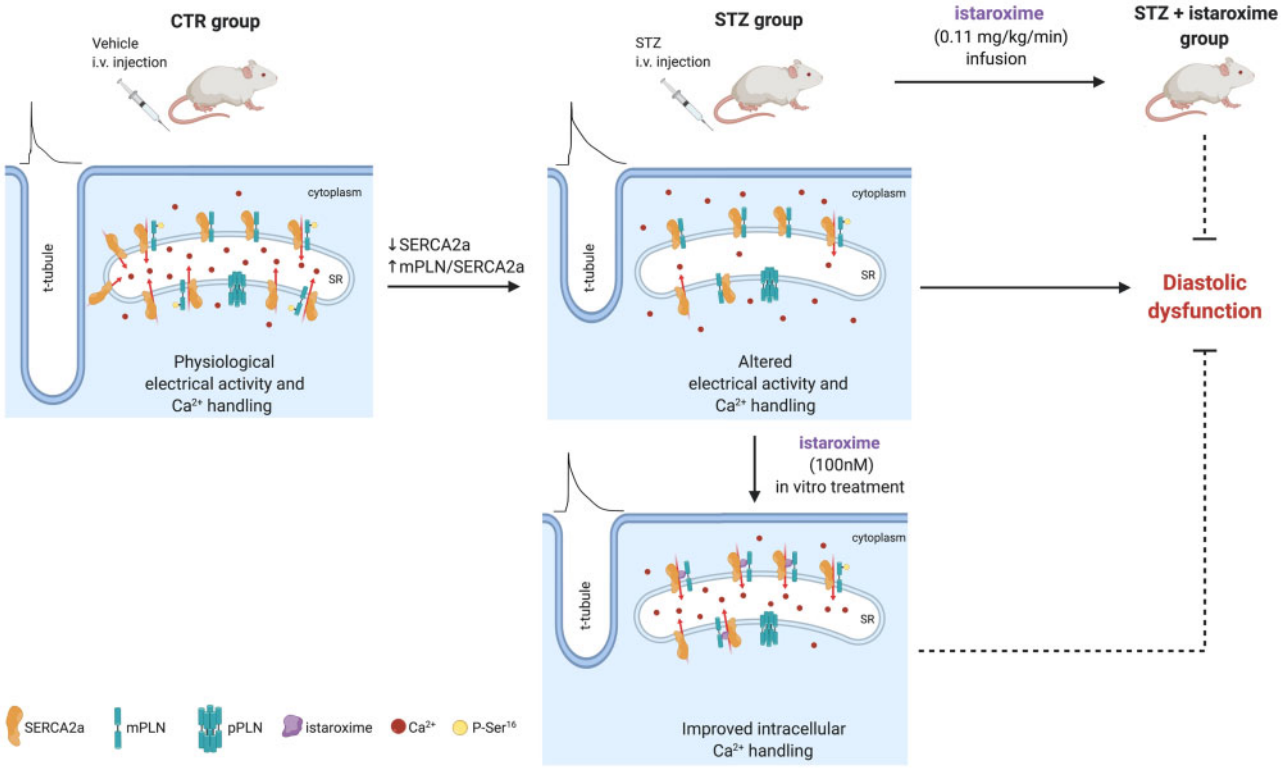

Keywords SERCA • Istaroxime • Diastolic dysfunction • Streptozotocin • Calcium handling

1. Introduction

Diabetes affects more than 300 million people globally and type 1 diabetes (T1D) accounts for up to 10% of cases.[1] Heart failure (HF) is the predominant cardiovascular complication of diabetes and represents the leading cause of morbidity and mortality. Diabetic cardiomyopathy (DCM) is a complex and multifactorial disease characterized by an early onset of diastolic dysfunction (DD), which precedes the development of systolic impairment.[2–5]

The molecular and pathophysiological mechanisms underlying diabetes include abnormalities in the regulation of Ca^{2+} homeostasis in cardiomyocytes and the consequent alteration of ventricular excitation–contraction coupling. In the diabetic heart, a dysregulation of Ca^{2+} cycling includes a reduction of SERCA2 activity, which may be accompanied by a decreased SERCA2 protein expression (mostly SERCA2a isoform).[6,7] A key role in the regulation of SERCA2a activity is played by phospholamban (PLN), a protein that behaves like its endogenous inhibitor when it is in its non-phosphorylated state.[8] In most diabetic models, PLN expression level appears increased while its phosphorylation state is reduced, thus, contributing to the inhibition of SERCA2a function.[6–8] This defect generates an impairment of sarcoplasmic reticulum (SR) Ca^{2+} refilling that results in slow diastolic relaxation. An abnormal Ca^{2+} distribution may facilitate cardiac arrhythmias appearance and myocyte apoptosis.[9,10]

Therefore, SERCA2a may represent a molecular target for a pharmacological intervention aimed at increasing the mechanical function and the energetic efficiency of the diabetic heart characterized by a defective SR Ca^{2+} loading. To date, the current medications have shown a limited efficacy in preventing the progression to HF in patients with DCM and diabetic complications.[10–12] New hypotheses have been recently proposed in HF aimed at improving cardiac contractility,[13–19] however, all these attempts are still far from being considered as beneficial treatment options available for clinicians and the treatment of HF and DCM remains an open field of research. The development of a small molecule as SERCA2a activator represents a promising strategy for HF and DCM treatment. Along this line, istaroxime is the first-in-class original luso-inotropic agent, shown to be highly effective and safe in patients.[20] Istaroxime is endowed of a double mechanism of action that consists in the ability to inhibit Na^+/K^+ ATPase (NKA) and enhance SERCA2a ATPase activity,[21] this last obtained through the relief of PLN inhibitory effect on SERCA2a,[22] without inducing spontaneous Ca^{2+} release (SCR) from SR.[21,23] In healthy and failing animal models and in patients with acute HF syndrome, istaroxime improves systolic and diastolic performance[20,24–28] and efficiency of cardiac contraction with a low oxygen consumption,[26] minimizing the risk of arrhythmias or ischaemia, without affecting other cardiovascular functions.[29–32]

In this study, we characterized the streptozotocin (STZ) model on different levels of biological organization, such as: (i) *in vivo*, to evaluate

STZ-induced DD, (ii) in isolated left ventricular (LV) cardiomyocytes, to evaluate structure, intracellular Ca^{2+} ($Ca^{2+}{}_i$) dynamics, electrical activity, and (iii) in LV and renal preparations (cell-free systems) to assess SERCA2a and NKA activity. We tested whether SERCA2a stimulation by a small molecule can improve the altered $Ca^{2+}{}_i$ handling responsible for the DD in STZ-treated rats. To this end, istaroxime was tested (i) *in vivo* after iv infusion in STZ rats, (ii) in LV myocytes at a concentration marginally affecting NKA to highlight its effects mostly dependent on SERCA2a stimulation, and (iii) in the cell-free systems.

2. Methods

All experiments involving animals (methods detailed in the online Supplementary material) conformed to the guidelines for Animal Care endorsed by the University of Milano-Bicocca and to the Directive 2010/63/EU of the European Parliament on the protection of animals used for scientific purposes. Male Sprague Dawley rats (150–175 gr) were used to generate a STZ-induced T1D cardiomyopathy model according to the Health Minister of Italy permission.

2.1 STZ rat model

T1D was induced through a single STZ (Sigma-Aldrich, 50 mg/kg) injection into a rat-tail vein; littermate control (CTR) rats received only citrate buffer (vehicle). Overnight fasting or non-fasting glycaemia was measured after 1 week by Contour XT system (Bayer). Animals were considered diabetic with fasting glycaemia values >290 mg/dL.

2.2 Echocardiography

Eight weeks after vehicle/STZ injection, rats were submitted to a transthoracic echocardiographic and Tissue Doppler evaluation, performed under urethane anaesthesia (1.25 g/kg i.p.) (M9 Mindray Echographer equipped with a 10 MHz probe, P10-4s Transducer, Mindray, China). Systolic and diastolic parameters were measured in CTR and diabetic (STZ) animals by a blinded investigator. Details are shown in the online Supplementary material.

A group of STZ rats was subjected to istaroxime infusion at 0.11 mg/kg/min for 15 min accordingly to a previous study.[25] Drug was infused through a polyethylene 50 cannula inserted into a jugular vein under urethane anaesthesia. Echocardiographic and Tissue Doppler parameters were measured under basal condition (before) and following 15 min istaroxime administration.

2.3 Morphometric parameters

Rats were euthanized by cervical dislocation under anaesthesia with ketamine-xylazine (130–7.5 mg/kg i.p) 9 weeks after STZ injection. Body weight (BW), heart weight (HW), LV weight (LVW), and kidney weight (KW) were measured. Body weight gain (BW gain) was obtained by subtracting the initial BW from the BW at sacrifice. HW and KW were normalized to tibia length (TL) to assess respectively cardiac and kidney indexes in CTR and STZ groups.

2.4 Myocyte dimensions and T-tubules (TT) analysis

Sarcolemmal membranes were stained by incubating isolated LV myocytes with 20 µmol/L di-3-ANEPPDHQ[33] (Life Technologies, Carlsbad, United States) to measure cell dimensions and TT organization/periodicity by a method based on Fast Fourier Transform.[34]

2.5 SERCA2a and Na^+/K^+ pump (NKA) activity measurement

SERCA2a activity was measured *in vitro* as ^{32}P-ATP hydrolysis at different Ca^{2+} concentrations (100–3000 nmol/L) in heart homogenates as previously described.[25] Ca^{2+} concentration–response curves were fitted by using a logistic function to estimate SERCA2a Ca^{2+} affinity (K_d Ca^{2+}) and V_{max}.

NKA activity was assayed *in vitro* by measuring the release of ^{32}P-ATP, as previously described.[35] The concentration of compound causing 50% inhibition of the NKA activity (IC_{50}) was calculated by using a logistic function.

2.6 Intracellular Na^+ and Ca^{2+} dynamics

Intracellular Na^+ ($Na^+{}_i$) and Ca^{2+} ($Ca^{2+}{}_i$) dynamics were evaluated by incubating LV myocytes with the membrane-permeant form of the dyes Ion NaTRIUM Green-2 AM (5 µmol/L) and Fluo4-AM (10 µmol/L), respectively.

$Na^+{}_i$ dynamics were monitored in I-clamp under physiological condition (Tyrode's solution) and in V-clamp under modified Tyrode's solution suitable to measure NKA current (I_{NKA}) at the same time.

$Ca^{2+}{}_i$ dynamics were analysed in field stimulated (2 Hz) and in patch-clamped myocytes. In field stimulated cells, SR Ca^{2+} loading and stability were evaluated through a post-rest potentiation protocol (Supplementary material online, *Figure S1*). Ca^{2+} transient (Ca_T) parameters and SR Ca^{2+} content (Ca_{SR}) were estimated at steady state (2 Hz) and following caffeine (10 mmol/L) superfusion, respectively. Moreover, incidence of SCR events was evaluated in each group during resting pauses and diastole.

To better highlight changes in $Ca^{2+}{}_i$handling not affected by modifications on electrical activity, $Ca^{2+}{}_i$ dynamic was also evaluated in voltage-clamped cells. Firstly, action potential (AP) clamp experiments were performed to verify whether Ca_T amplitude and Ca_{SR} were dependent on AP durations (APDs). To this end, two AP waveforms were used to dynamic voltage clamp STZ myocytes: a 'short AP' and a 'long AP' representative of the CTR and STZ group in terms of AP characteristics, respectively. $Ca^{2+}{}_i$ dynamics were then evaluated in voltage-clamped cells by standard V-clamp protocols.

Finally, to estimate SR uptake function in the absence of Na^+/Ca^{2+} exchanger (NCX) and NKA function, SR reloading protocol was applied in V-clamped cells by removing Na^+ from both sides of the sarcolemma (Supplementary material online, *Figure S2*).[21] Kinetics of SR Ca^{2+} reloading was evaluated; in particular, we considered the time constant of Ca_T decay (τ_{decay}) reflecting in this setting Ca^{2+} transport rate across the SR membrane, a functional index of SERCA2a activity.

2.7 Ca^{2+} sparks rate and characteristics

Spontaneous unitary Ca^{2+} release events (Ca^{2+} sparks) were recorded at room temperature in Fluo 4-AM (10 µmol/L) loaded myocytes at resting condition. Tyrode's bath solution contained 1 mmol/L $CaCl_2$.

2.8 AP rate-dependency and variability

APs were recorded in I-clamp condition by pacing myocytes at 1, 2, 4, and 7 Hz under Tyrode superfusion. Rate-dependency of APD at 50% (APD_{50}) and 90% (APD_{90}) of repolarization and diastolic potential (E_{diast}) were evaluated at steady state. Moreover, at each rate, a minimum of 30 APs were recorded at steady state to evaluate the short-term variability (STV) of APD_{90}, a well-known pro-arrhythmic index,[36] according to Eq. (1):

$$STV = \sum(|APD_{(n+1)} - APD_n|)/[n_{beats} \times \sqrt{2}] \quad (1)$$

Incidence of delayed afterdepolarizations (DADs) was evaluated.

2.9 Statistical analysis

Normal distribution of the results was checked by using the Shapiro–Wilk test. Paired or unpaired Student's *t*-test, one-way or two-way ANOVA were applied as appropriate test for significance between means. *Post hoc* comparison between individual means was performed by Tukey or Sidak multiple comparison tests. χ^2 test was used for comparison of categorical variables. Results are expressed as mean ± SEM. A value of $P < 0.05$ was considered significant.

Except when specified, *in vitro* istaroxime effects were analysed by incubating cells with the drug for at least 30 min, thus group comparison analysis was performed. Number of animals (*N*) and cells (*n*) are shown in each figure legend.

3. Results

3.1 Morphometric parameters

Diabetic rats were obtained by a single injection of STZ (50 mg/kg) into a tail vein and were compared to CTR rats receiving only vehicle. Fasting and non-fasting glycaemia increased significantly 1 week after STZ administration (*Table 1*).

At the time of STZ administration, BW was comparable among CTR and STZ groups (data not shown), while 9 weeks after STZ infusion, BW gain was largely different among groups because of a BW significantly lower in STZ than in CTR. TL was also measured as a rat growth index and resulted slightly reduced in STZ compared to CTR. HW was significantly lower in STZ than in CTR, even when HW was normalized to TL. Analogously, LVW normalized to HW, was significantly reduced in STZ in comparison to CTR. Likewise, LV cell length, volume, cross-sectional area (CSA), and cell membrane capacitance (C_m), a further index of cell dimension, were significantly reduced in STZ in comparison to CTR. Conversely, KW did not differ between the two groups, but KW/TL ratio resulted modestly increased in STZ rats vs. CTR, suggesting STZ-induced kidney hypertrophy (*Table 1*).

Table 1 Glycaemia values, morphometric parameters, and LV cell dimensions

	CTR	STZ	*P* vs. CTR
Fasting glycaemia (mg/dL)	94±2	390±14	*
Non-fasting glycaemia (mg/dL)	126±4	560±8	*
BW (g)	400±7	202±6	*
BW gain (g)	230±14	26±8	*
HW (g)	1.65±0.08	1.03±0.03	*
TL (cm)	4.3±0.02	3.63±0.03	*
HW/BW (g/kg)	4.11±0.17	5.16±0.11	*
HW/TL (g/cm)	0.40±0.03	0.28±0.009	*
LVW/HW (%)	67.9±1.0	63.4±0.7	*
KW (g)	2.23±0.05	2.19±0.07	NS
KW/TL (g/cm)	0.52±0.01	0.6±0.02	*
LV cell length (μm)	136±2.8	120±2.1	*
LV cell volume (10^3 μm^3)	65±1.9	37±1.03	*
LV CSA (um^2)	482±13.8	309±7.5	*
LV C_m (pF)	179±6	136±4	*

BW, Body weight; HW, heart weight; KW, kidney weight; LVW, left ventricular weight; TL, tibia length.
Morphometric parameters: CTR *N* =15–21, STZ *N* =23–34. Cell dimensions (length, volume, and CSA): CTR *N* =4 (*n* =58), STZ *N* =6 (*n* =108). Cell membrane capacitance (C_m): CTR *N* =12 (*n* =75), STZ *N* =13 (*n* =83).
*P<0.05 vs. CTR (unpaired *t*-test).

It was further investigated whether the decrease of cardiac weight/mass observed in STZ rats might be associated with cardiac fibrosis deposition. To this end, a western blot analysis for collagen type 1 and matrix metallopeptidase 9 (MMP-9) protein expression level was conducted on LV homogenates from CTR and STZ rats (Supplementary material online, *Figure S3*). The results indicate that any significant difference of collagen type 1 and MMP-9 protein content could be detected between the two rat groups.

3.2 STZ induces DD, reverted by acute istaroxime infusion

The echocardiographic parameters were measured in CTR and STZ rats 8 weeks after STZ injection (*Table 2*). Wall thickness for the interventricular septum (IVST) and posterior wall (PWT) both in diastole and systole did not differ between CTR and STZ rats. Analogously, LV end-diastolic and systolic diameter (LVEDD, LVESD) remained unchanged. The calculated fractional shortening (FS) did not differ while the TDI contraction velocity (s') was reduced in STZ animals when compared to CTR, thus suggesting an overall systolic function only partially compromised in STZ rats at this stage (*Table 2*).

The transmitral Doppler parameters were altered in STZ rats indicating an impairment of diastolic function. In particular, in STZ rats, while early (E) peak diastolic velocity was unchanged, E wave deceleration time (DT) was prolonged, thus, the mitral deceleration index (DT/E) and the deceleration slope (E/DT) tended respectively to increase and decrease; late peak diastolic velocity (A) was significantly increased and thus, E/A ratio resulted significantly reduced. Tissue Doppler examination showed in STZ rats a significant reduction of early diastolic myocardial velocity (e') and a significant increase of late diastolic myocardial velocity (a'), similarly to A wave. Thus, a significant reduction of e'/a' ratio and increase of the E/e' ratio was observed in STZ rats in comparison to CTR (*Table 2*).

The overall cardiac function indicated that stroke volume (SV), ejection fraction (EF), and cardiac output (CO) were not significantly affected in STZ rats although heart rate (HR) was reduced. Echocardiographic data mostly indicate that, at this time point, STZ induced a DCM characterized by DD and mostly preserved systolic function. Furthermore, the diastolic impairment observed in STZ rats at this early stage was not associated with cardiac fibrosis (Supplementary material online, *Figure S3*).

To analyse early *in vivo* effects of istaroxime in reducing STZ-induced DD, istaroxime was infused in STZ rats at 0.11 mg/kg/min[25] and echocardiographic parameters were collected 15 min later. The results (*Table 2*) showed that the compound was able to revert the DD documented in STZ rats with a significant reduction of DT and DT/E and an increase of E/DT and e'. No effect on CO, SV, and HR was observed following istaroxime infusion at this early time point (*Table 2*). Moreover, to exclude changes due to time dependent effects of urethane, echocardiographic parameters were collected every 5 min in a set of animals not treated with the drug. Up to 20 min in urethane anaesthesia, diastolic and systolic parameters remained constant (Supplementary material online, *Figure S4*). It should be noted that in a parallel study, we estimated istaroxime

Table 2 Echocardiographic and tissue Doppler parameters

	CTR	STZ basal	STZ + istaroxime
IVSTd (mm)	1.9±0.09	1.81±0.12	1.88±0.12
PWTd (mm)	1.71±0.17	1.45±0.08	1.47±0.07
LVEDD (mm)	6.6±0.35	7.08±0.32	7.27±0.23
IVSTs (mm)	2.6±0.22	2.54±0.18	2.57±0.19
PWTs (mm)	2.71±0.2	2.52±0.1	2.55±0.21
LVESD (mm)	3.07±0.39	3.11±0.28	3.1±0.34
FS (%)	53.8±5.66	56.2±2.4	57.7±3.7
E (m/s)	0.88±0.03	0.89±0.05	0.95±0.05
A (m/s)	0.52±0.07	0.7±0.03*	0.81±0.05**
E/A	1.82±0.21	1.26±0.03*	1.18±0.05
DT (ms)	53.5±1.55	61±2.17*	48.4±3.8**
DT/E (10^{-3} s^2/m)	61.3±1.43	69.3±4.5	52.2±5.6**
E/DT (10^3 m/s^2)	16.3±0.35	14.7±0.9	20.8±2.8**
s' (mm/s)	33.2±1.18	24.8±1.19*	25.2±1.11
e' (mm/s)	26.7±1.73	21.2±0.63*	24.5±1.46**
a' (mm/s)	20.7±1.61	27.8±1.99*	31.1±2
e'/a'	1.31±0.063	0.77±0.03*	0.79±0.02
E/e'	33.2±1.56	42.3±2.43*	39.1±1.57
HR (bpm)	303±9.5	233±10*	240±13
SV (mL)	0.59±0.1	0.73±0.08	0.78±0.05
CO (mL/min)	179.8±30.3	170.2±17	186.9±15
EF (%)	83.6±3.2	89.9±1.6	90.2±2.3
N	7	7	7

Average values in CTR and STZ animals before (basal) and after infusion with istaroxime at 0.11 mg/kg/min for 15 min.
A, a', late diastolic peak velocity; CO, cardiac output; DT, deceleration time; E, e', early diastolic peak velocity; EF, ejection fraction; FS, fractional shortening; HR, heart rate; IVSTd, telediastolic interventricular septum thickness; IVSTs, telesystolic interventricular septum thickness; LVEDD, left ventricular early-diastolic diameter; LVESD, left ventricular early-systolic diameter; PWTd, telediastolic posterior wall thickness; PWTs, telesystolic posterior wall thickness; s', systolic peak velocity; SV, stroke volume.
*P<0.05 vs. CTR (unpaired t-test),
**P<0.05 vs. STZ basal (paired t-test). CTR N=7, STZ N=7.

plasma level in male rats after 1 hour infusion at 0.11 mg/kg/min, resulting 780 nmol/L (N = 3, unpublished data); this suggests that drug concentration at 15 min infusion should be reasonably around 200 nmol/L.

3.3 Istaroxime affinity for rat NKA

To identify the *in vitro* istaroxime concentration suitable to limit its effects dependent on NKA inhibition, I_{NKA} was isolated in CTR rat LV myocytes and the concentration–response curve for istaroxime was evaluated as previously shown for guinea-pig[30] and mouse myocytes.[23] A saturating concentration of ouabain (1 mmol/L) was used (Supplementary material online, *Figure S5*) to evaluate the I_{NKA} inhibition by istaroxime as percentage of the ouabain-induced change. Moreover, a subgroup of cells was incubated with Ion NaTRIUM Green-2 to monitor Na^+_i changes under istaroxime or ouabain superfusion. The estimated IC_{50} for I_{NKA} inhibition by istaroxime was 32 ± 4 µmol/L (*Figure 1A*); a similar value was detected in cardiac (84 ± 20 µmol/L) (inset *Figure 1A*) and renal preparations (55 ± 19 µmol/L, Supplementary material online, *Figure S6*). Moreover, while NKA inhibition by 100 nmol/L istaroxime was detectable by measuring I_{NKA} in isolated myocytes (-6.9 ± 1.2%, P < 0.05, N = 14), istaroxime effects on NKA were not detectable up to 1 µmol/L in cardiac and renal preparations.

In isolated rat ventricular myocytes Na^+_i increased slightly under cumulative istaroxime concentrations (20 µmol/L istaroxime +2.2 ± 0.7%, P < 0.05, N = 5), while it was evident under saturating ouabain concentration (+8 6 ± 1.4%, P < 0.05, N = 5) (*Figure 1A*).

Consistently with the aim of the study, istaroxime effects on STZ-induced changes were evaluated by testing the compound at concentrations marginally affecting NKA (100 or 500 nmol/L).

3.4 STZ induces SERCA2a down-regulation and TT loss

LV homogenates from CTR and STZ rats were used to measure SERCA2a and PLN protein level by western blot analysis. Representative western blots from CTR and STZ samples and the relative densitometric analysis indicized for actin content are shown in *Figure 1B*. SERCA2a protein expression resulted significantly reduced in STZ vs. CTR samples (-45%, P < 0.001); while monomeric (m) PLN levels were unchanged, pentameric (p) PLN levels were slightly increased (+22%, P < 0.05). As a consequence, both mPLN/SERCA2a and pPLN/SERCA2a ratio were significantly increased (+89% and +128%, respectively, P < 0.001), suggesting higher SERCA2a inhibitory activity by PLN in STZ group. Moreover, in STZ samples, while the fraction of phosphorylated Thr^{17}-mPLN (pThr^{17}-mPLN/mPLN) resulted unchanged, the fraction of phosphorylated Ser^{16}-mPLN (pSer^{16}-mPLN/mPLN) was reduced (-42%, P < 0.05), thus highlighting reduced PKA-dependent SERCA2a modulation in STZ. Most of these measurements were also performed in isolated LV myocytes showing comparable results as those shown in LV homogenates (Supplementary material online, *Figure S7*).

SERCA2a activity was measured in cardiac SR homogenates from CTR and STZ rats as ^{32}P-ATP hydrolysis assay (*Figure 1C*). In comparison to CTR preparations, SERCA2a V_{max} was significantly decreased (-25%, P < 0.05) in STZ, while the K_d Ca^{2+} did not differ (Supplementary material online, *Figure S8*). Overall, SERCA2a protein level and activity were reduced in STZ preparations, a result in line with echocardiographic parameters showing STZ-induced DD.

Disarray of the TT system has been described in several failure models and was generally characterized by loss of the transverse component. A sharp pattern of transverse striations was observed in CTR myocytes (*Figure 1D*); accordingly, in these myocytes, pixel variance was largely represented by the periodic component, whose period was consistent with transverse TT arrangement. LV disarray of the transverse TT was visually obvious in STZ myocytes, a result confirmed by the quantitative analysis of the power of the periodic component (*Figure 1D*).

3.5 Istaroxime effects on STZ-induced changes in Ca^{2+} dynamics

Istaroxime (500 nmol/L) stimulated SERCA2a activity in cardiac SR homogenates from STZ diabetic rats by increasing SERCA2a V_{max} (+25%, P < 0.01) to a value similar to CTR rats (*Figure 1C*) without affecting the K_d Ca^{2+} affinity (575 ± 98 nmol/L vs. 450 ± 51 nmol/L, NS, Supplementary material online, *Figure S8*). Conversely, in CTR rat preparations, V_{max} (*Figure 1C*) and K_d Ca^{2+}(Supplementary material online, *Figure S8*) parameters were unchanged in the presence of istaroxime.

Istaroxime effects on STZ-induced DD were then evaluated at the cellular level by measuring the SR ability to accumulate resting Ca^{2+} through a post-rest potentiation protocol in field stimulated myocytes. As shown in *Figure 2A*, following increasing resting pauses, the amplitude of the first

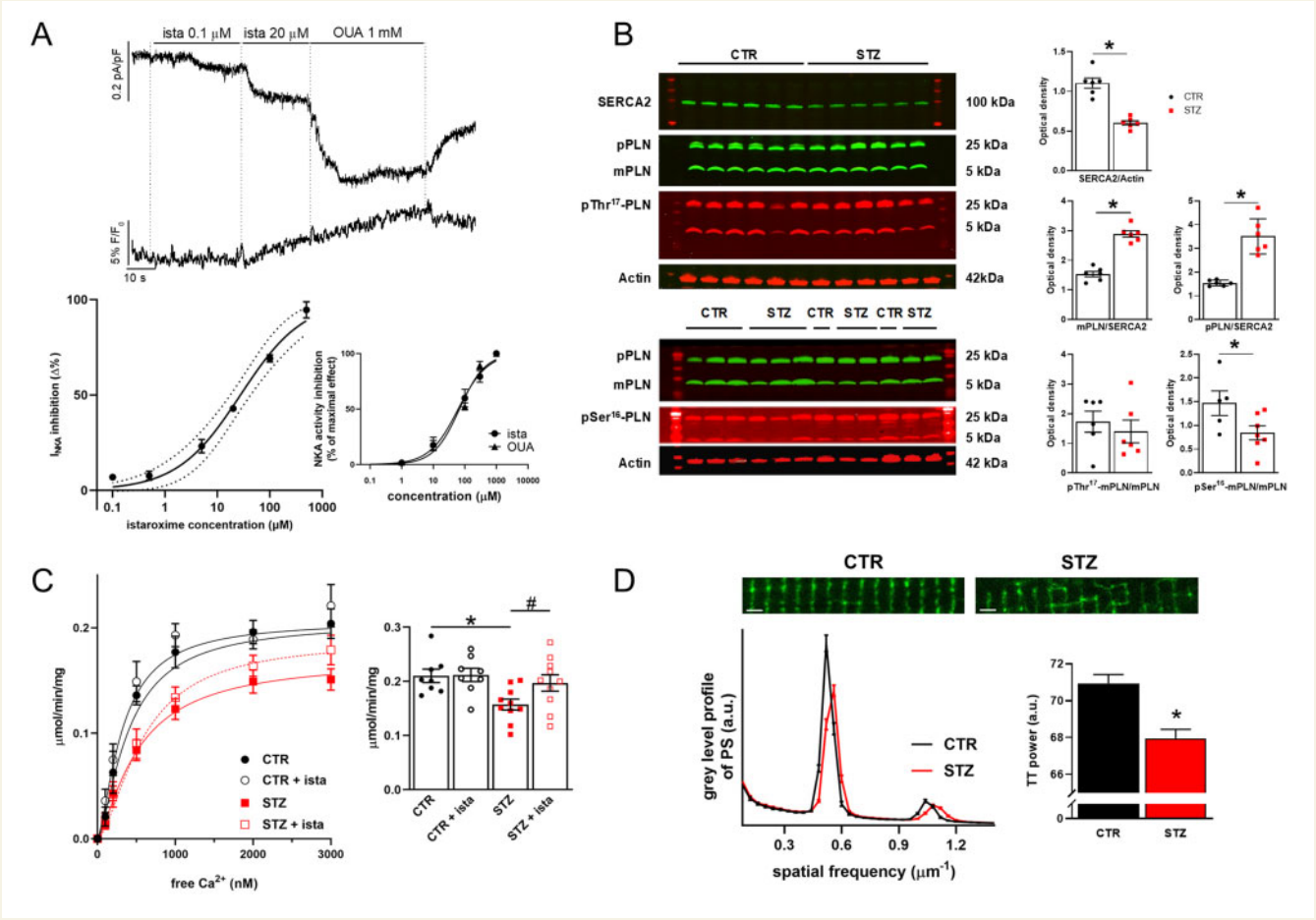

Figure 1 Istaroxime affinity for rat NKA. Changes in SERCA2, PLN levels, and TT expression in STZ vs. CTR rats. (*A*) Top: recordings of NKA current (I_{NKA}) and Ion NaTRIUM Green-2 fluorescence (Hp -40 mV) during exposure to increasing concentrations of istaroxime and, finally, to 1 mmol/L ouabain (OUA). Bottom: concentration-dependent I_{NKA} inhibition by istaroxime in isolated CTR LV myocytes (the best logistic fit and confidence intervals are shown, $N = 5$, $n = 6–27$). Concentration-dependent NKA activity inhibition by istaroxime and OUA in cardiac preparations is shown in the inset ($N = 5$). (*B*) Left: western blot for SERCA2, monomeric (m) and pentameric (p) PLN, pSer^{16}-PLN and pThr^{17}-PLN in STZ ($N = 6,7$) and CTR ($N = 5,6$) cardiac homogenates. Right: densitometric analysis; values are expressed as optical density in arbitrary units. *P<0.05 vs. CTR (unpaired t-test). (*C*) Left: Ca^{2+} activation curves of SERCA2a activity measured as cyclopiazonic acid sensitive component in cardiac SR homogenates from CTR ($N = 8$) and STZ ($N = 10$) rats with or w/o 500 nmol/L istaroxime. Right: statistics of the maximum velocity (V_{max}) of the Ca^{2+} activation curves estimated by sigmoidal fitting. *P<0.05 vs. CTR (unpaired t-test), #P<0.05 vs. STZ (paired t-test). (D) Top: confocal images of di-3-ANEPPDHQ (20 μmol/L) loaded CTR and STZ myocytes (horizontal bars 2 μm). Bottom: mean power spectrum profile of TT in CTR ($N = 5$, $n = 114$) and STZ ($N = 9$, $n = 181$) group; average results of the power of the periodic component on the right. *P<0.05 vs. CTR (unpaired t-test).

Ca_T increased progressively in CTR myocytes; according to STZ-induced SERCA2a down-regulation, post-rest potentiation was reduced in STZ myocytes at all resting intervals. Istaroxime at 100 nmol/L failed to affect post-rest potentiation in CTR myocytes, while it improved the ability of SR to accumulate Ca^{2+} especially at long resting pauses in STZ myocytes, in agreement with its stimulatory action on SERCA2a.

At steady-state, STZ increased diastolic Ca^{2+} (Ca_D) and CaT decay time ($t_{0.5}$), while leaving unchanged Ca_T amplitude and Ca_{SR} (*Figure 2B and C*). Istaroxime (100 nmol/L) significantly increased Ca_D in CTR myocytes, while blunted STZ-induced Ca_D enhancement in STZ myocytes. This was furtherly appreciable monitoring the time course of Ca_D enhancement during the SR reloading process following caffeine superfusion (*Figure 2D*). On the other hand, Ca_T amplitude, decay kinetics, and Ca_{SR} were not significantly affected by istaroxime in both CTR and STZ myocytes. Overall, STZ-induced SERCA2a down-regulation resulted in cytosolic Ca_D enhancement probably due to a reduced ability of SR to compartmentalize Ca^{2+} into the SR; however, SR Ca^{2+} content was preserved. In parallel, the effect of istaroxime on Ca_D in CTR myocytes was likely attributable to a partial NKA blockade, that was blunted in STZ myocytes by the simultaneous action on SERCA2a.

SCR events were evaluated in CTR and STZ cells. SCR events were absent in CTR while a not significant number of events occurred in STZ myocytes; istaroxime not affected their incidence in both CTR and STZ myocytes.

3.6 STZ induces changes in electrical activity affecting Ca^{2+}_i dynamics. Analysis of istaroxime effects

Potential changes in electrical activity in STZ myocytes might mask expected changes directly resulting from SERCA2a down-regulation (e.g. changes in Ca_{SR}).

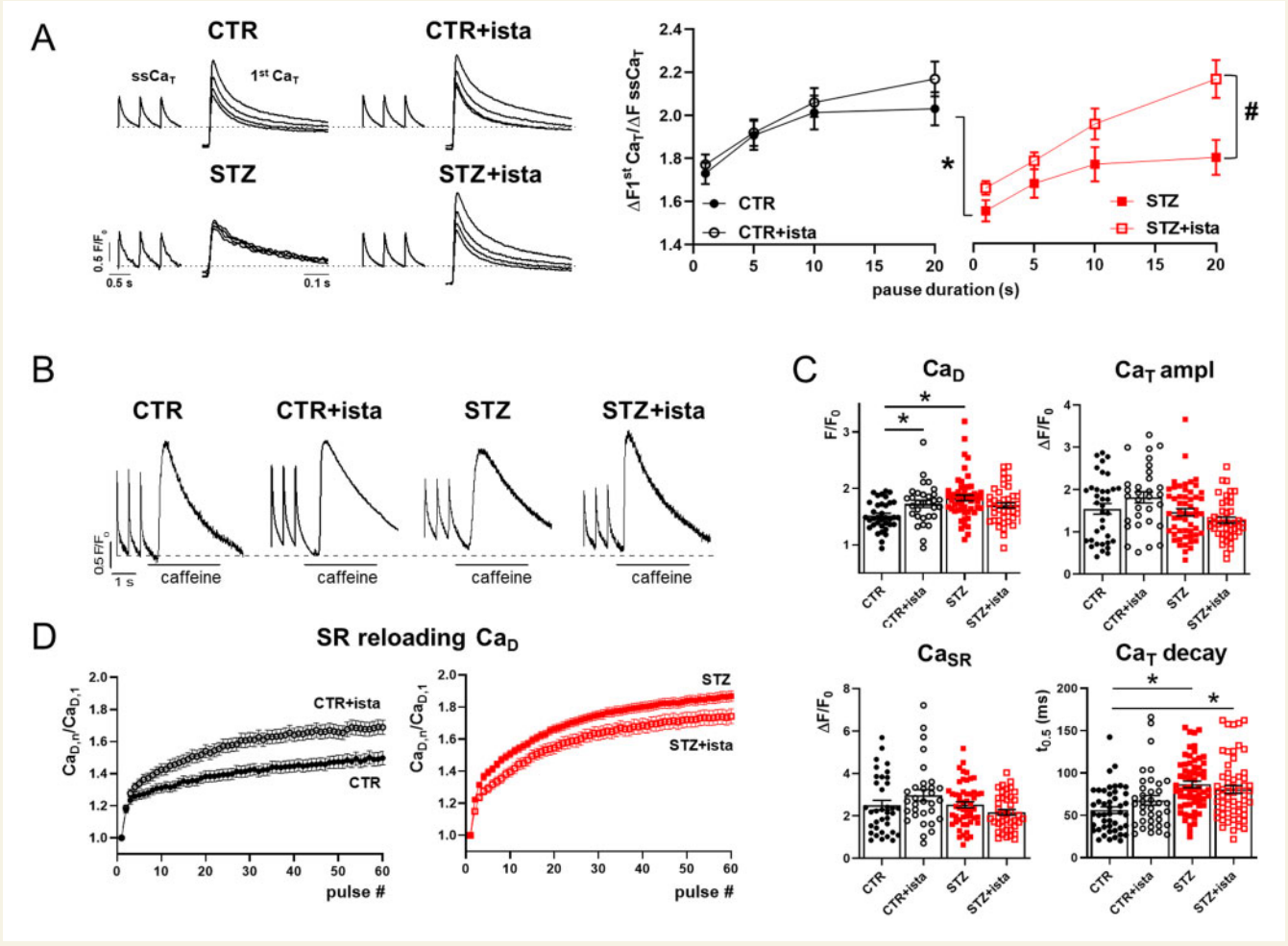

Figure 2 STZ-induced changes in Ca_i^{2+} dynamics in field stimulated myocytes. Analysis of istaroxime effects. (*A*) Left: post-rest potentiation protocol in Fluo4 field stimulated (2 Hz) myocytes; steady state Ca^{2+} transients ($ssCa_T$) and superimposed first Ca^{2+} transients (1^{st} Ca_T) following increasing resting pauses (1–5–10–20 s) are reported in CTR and STZ myocytes, with or w/o 100 nmol/L istaroxime. Traces were normalized to own diastolic Ca^{2+} (Ca_D) level (dotted lines). Right: analysis of the 1^{st} Ca_T amplitude normalized to the amplitude of the pre-pause $ssCa_T$ and its pause-dependency. CTR N = 5 (w/o istaroxime n = 44, with istaroxime n = 34), STZ N = 3 (w/o istaroxime n = 35, with istaroxime n = 23). *P<0.05 vs. CTR w/o istaroxime; #P<0.05 vs. STZ w/o istaroxime (two-way ANOVA plus *post hoc* Sidak's multiple comparisons). (*B*) $ssCa_T$ and caffeine-induced Ca_T evocated in field stimulated CTR and STZ myocytes with or w/o 100 nmol/L istaroxime (the dotted line indicates the Ca_D in CTR w/o istaroxime). (*C*) Statistics for $ssCa_D$, $ssCa_T$ amplitude, caffeine-induced Ca_T (named Ca_{SR}), and $ssCa_T$ half decay time ($t_{0.5}$). CTR N = 5 (n = 36 w/o istaroxime, n = 31 with istaroxime), STZ N = 7 (n = 52 w/o istaroxime, n = 42 with istaroxime). *P<0.05 vs. CTR w/o istaroxime (one-way ANOVA plus *post hoc* Tukey's multiple comparisons). (*D*) Changes in Ca_D during the reloading process after caffeine-induced SR depletion. Ca_D values ($Ca_{D,n}$) were normalized to the 1^{st} pulse Ca_D ($Ca_{D,1}$). CTR N = 5 (n = 36 w/o istaroxime, n = 29 with istaroxime), STZ N = 7 (n = 49 w/o istaroxime, n = 43 with istaroxime).

Thus, to verify STZ-induced changes in electrical activity, AP rate-dependency was evaluated in STZ myocytes in comparison to CTR. STZ induced a significant APD prolongation at all stimulation rates (*Figure 3A*), accordingly to voltage-dependent K^+ channels down-regulation.[37,38] Moreover, rate-dependency of E_{diast} observed in CTR myocytes was absent in STZ myocytes, probably due to STZ-induced NKA down-regulation.[39] In both CTR and STZ myocytes, istaroxime at 100 nmol/L not affected APD, while slightly depolarized E_{diast} especially in STZ myocytes (*Figure 3A*).

All these measurements were done following istaroxime incubation for at least 30 min to allow drug accumulation inside the cell and stimulate SERCA2a. On the other hand, to better understand drug effects on E_{diast}, likely attributable to NKA inhibition, a group of CTR myocytes were loaded with Ion NaTRIUM Green-2 and membrane potential plus Na^+_i were simultaneously recorded at 7 Hz (to highlight the contribution of NKA to E_{diast}) under basal condition and following istaroxime (100 nmol/L) superfusion; ouabain at saturating concentration was also tested as reference compound inhibiting NKA (*Figure 3B*). Istaroxime at 100 nmol/L slightly depolarized E_{diast} (Δ-0.58 ± 0.1 mV, n = 8, P < 0.05) in comparison to ouabain superfusion (Δ-13.5 ± 1.2 mV, n = 13, P < 0.05); in parallel, a significant Na^+_i enhancement was detectable during ouabain only (+3 ± 0.5% n = 13, P < 0.05).

Overall, as expected, STZ treatment largely affects ion channels and pumps resulting in AP shape changes; istaroxime at 100 nmol/L substantially leaved unchanged STZ-induced AP changes and further slightly depolarized E_{diast}, resulting from a minimal (about -7%) NKA inhibition.

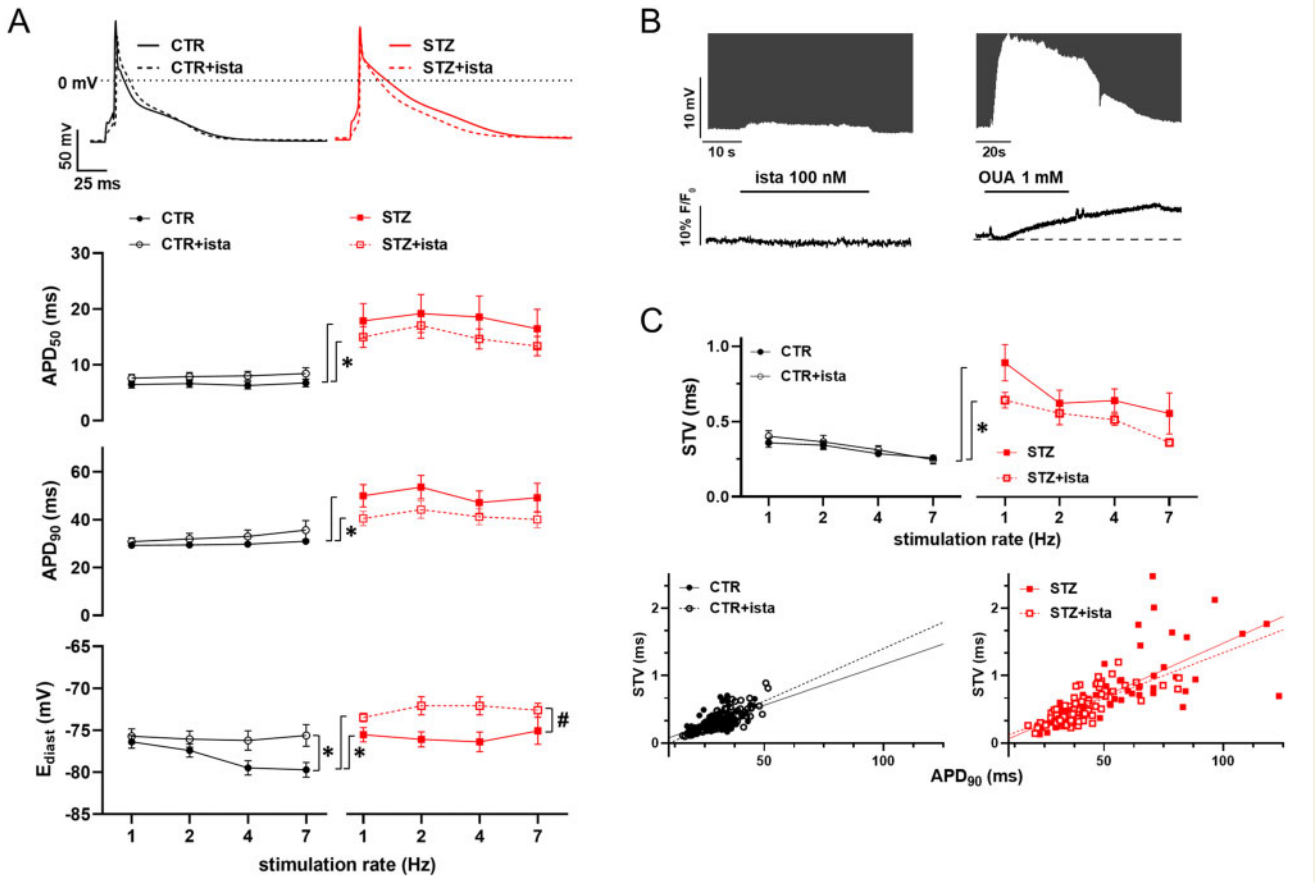

Figure 3 STZ-induced changes in electrical activity. Analysis of istaroxime effects. (*A*) Top: representative AP recorded at 1 Hz in CTR and STZ myocytes with or w/o 100 nmol/L istaroxime. Bottom: rate-dependency of AP parameters (APD_{50}, APD_{90}, E_{diast}) in CTR and STZ myocytes with or w/o 100 nM istaroxime. CTR $N = 4$ ($n = 29$ w/o istaroxime, $n = 25$ with istaroxime), STZ $N = 3$ ($n = 24$ w/o istaroxime, $n = 19$ with istaroxime). *$P<0.05$ vs. CTR w/o istaroxime, #$P<0.05$ vs. STZ w/o istaroxime (two-way ANOVA plus *post hoc* Sidak's multiple comparisons). (*B*) Effects of 100 nmol/L istaroxime superfusion on E_{diast} (top, AP *y* axis zoomed to highlight changes) and Na_i^+ (bottom) in comparison to the effect of 1 mmol/L OUA in CTR myocytes loaded with Ion Natrium Green-2 and stimulated at 7 Hz. (*C*) Top: rate-dependency of APD_{90} STV in each experimental group. CTR $N = 4$ ($n = 27$ w/o istaroxime, $n = 21$ with istaroxime), STZ $N = 3$ ($n = 24$ w/o istaroxime, $n = 20$ with istaroxime). *$P<0.05$ vs. CTR w/o istaroxime (two-way ANOVA plus *post hoc* Sidak's multiple comparisons). Bottom: linear correlation between STV of APD_{90} and APD_{90} values in CTR and STZ groups; data from all stimulation rates were pooled.

The STV of APD was evaluated in all groups, as a well-known pro-arrhythmic index. In comparison to CTR, STZ increased STV of APD at all pacing rates (*Figure 3C*); in both CTR and STZ myocytes, STV was not significantly affected by istaroxime, even though tended to be reduced in STZ myocytes. As expected, STV was directly correlated to APD_{90} in all groups; the slope of this correlation tended to increase in STZ group without reaching statistical significance (0.016 vs. 0.012, NS) and it was not significantly affected by istaroxime in both groups. These results suggest the absence of major mechanisms other than APD prolongation significantly affecting STV in all groups.[37]

Likewise to SCR incidence, DADs were completely absent in CTR myocytes and were present only in few cells in STZ groups (data not shown).

Given the STZ-induced APD prolongation, we verified if APD could effectively affect Ca^{2+}_i handling in STZ myocytes. To this end, AP-clamp measurements were performed (*Figure 4A*). Ca_T were evocated in the same cell by using as voltage commands waveforms named 'short' AP (CTR AP) and 'long' AP (STZ AP) (see Section 2). In comparison to the short AP waveform, the long AP one caused a huge increase in Ca_T amplitude (+66 ± 9.4%, $P < 0.05$) and Ca_{SR} (+36 ± 9.8%, $P < 0.05$), confirming the hypothesis that the prolonged AP in STZ myocytes affected Ca^{2+}_i handling.

3.7 STZ-induced Ca^{2+}_i handling changes under control of membrane potential are reverted by istaroxime SERCA2a stimulation

To clarify direct effects of SERCA2a down-regulation and its stimulation by istaroxime on Ca^{2+}_i handling, analysis on voltage-clamped myocytes was performed (*Figure 4B*) through a standard V-clamp protocol. Cells were superfused with Tyrode's solution to allow evaluation of both SR and NCX function. As shown in *Figure 4B*, STZ induced Ca_T and Ca_{SR} amplitude reduction, leaving unchanged fractional release. Influx through L-

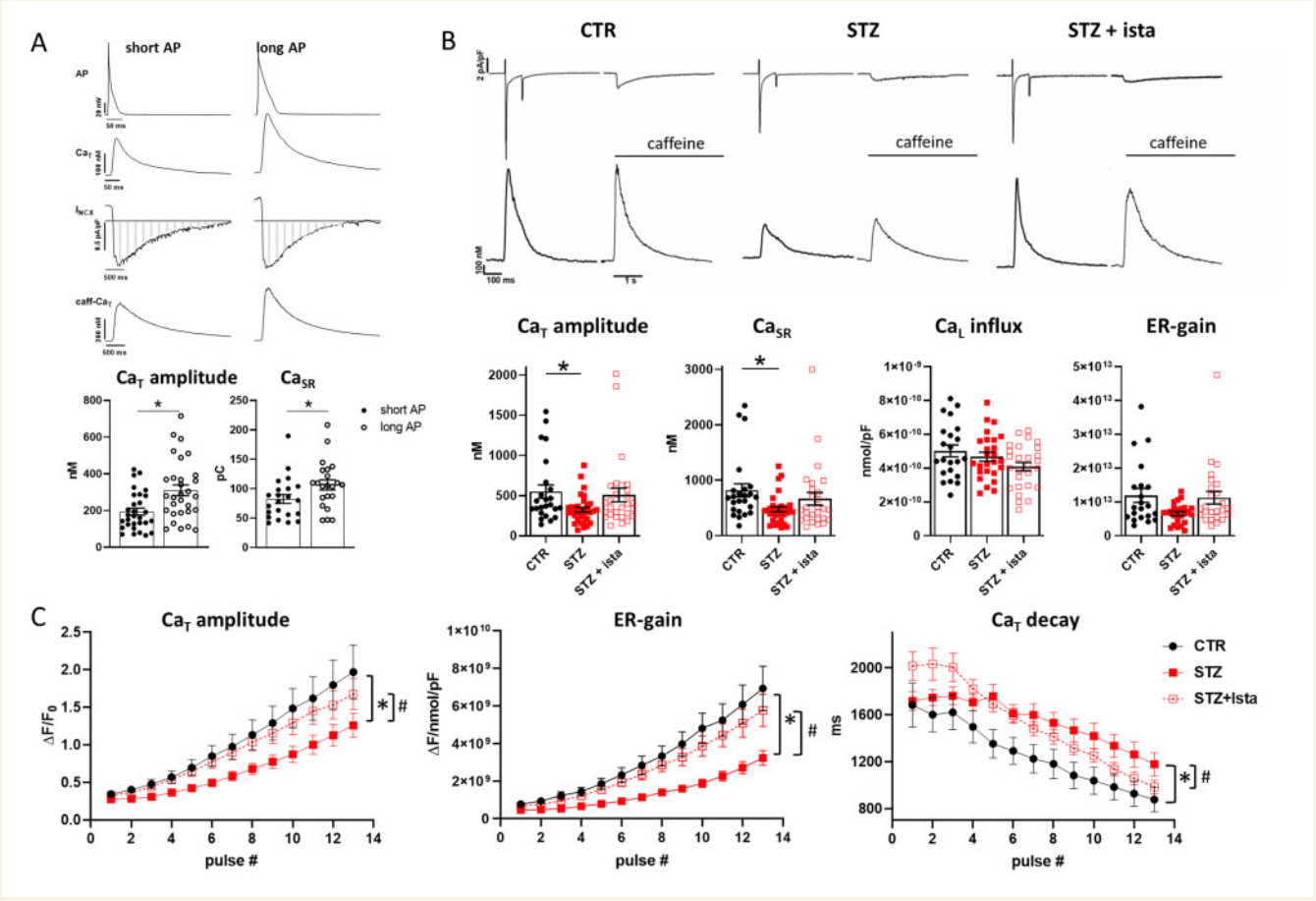

Figure 4 STZ-induced Ca_i^{2+} handling changes under control of membrane potential. Analysis of istaroxime effects. (*A*) Top: APs waveforms (CTR and STZ APs named short and long APs, respectively) and corresponding Ca_T evocated in V-clamped STZ myocyte through AP-clamp experiments (2 Hz). Caffeine-induced Ca_T (caff-Ca_T) and the corresponding NCX current (I_{NCX}) were recorded at -80 mV following steady state stimulation with short and long AP to estimate changes in SR Ca^{2+} content (Ca_{SR}). Bottom: statistics of Ca_T amplitude (N = 5, n = 30) and Ca_{SR} (integral of inward I_{NCX}, marked as striped area) (N = 5, n = 22) under short and long AP stimulation. Fluorescence signals were converted to free Ca^{2+} estimating F_{max} in each cell. *P<0.05 vs. short AP (paired t-test). (*B*) Top: transmembrane currents and Ca_T simultaneously recorded in voltage-clamped cells (Hp -35 mV) from CTR and STZ myocytes with or w/o 100 nmol/L istaroxime. Bottom: statistics of Ca_T amplitude, Ca_{SR}, Ca^{2+} influx through L-type Ca^{2+} channel (Ca_L influx), and ER gain. CTR N = 3 (n = 22–24), STZ N = 5 (w/o istaroxime n = 26–33, with istaroxime n = 28). Fluorescence signals were converted to free Ca^{2+} estimating F_{max} in each cell. *P<0.05 vs. CTR (one-way ANOVA plus Tukey's multiple comparison). (*C*) Statistics of Ca_T parameters (CaT amplitude, ER-gain, and CaT decay time constant) measured during each pulse after SR depletion under NCX blockade (see Supplementary material online, *Figure S2*) in CTR and STZ myocytes with or w/o 100 nmol/L istaroxime. *P<0.05 vs. CTR; #P<0.05 vs. STZ w/o istaroxime (two-way ANOVA); CTR N = 5 (n = 13–21), STZ N = 4 (w/o istaroxime n = 13–28, with istaroxime n = 19–24).

type Ca^{2+} channels (Ca_L influx) was not affected in STZ group, leading to an excitation–release (ER) gain that tended to be reduced in comparison to CTR. Moreover, in STZ myocytes, I_{CaL} peak density at 0 mV was significantly reduced, but the current decay tended to be slower; in particular, the fast decay time constant (τ_{fast}), reflecting Ca^{2+}-dependent inactivation, tended to increase in comparison to CTR myocytes (Supplementary material online, *Figure S9*). Thus, all I_{CaL} changes justify a global unaltered Ca^{2+} influx in STZ myocytes under these settings. Finally, the slope of the linear correlation between NCX current (I_{NCX}) and the Ca_{SR} ($\Delta I_{NCX}/\Delta Ca_{SR}$) was similar in CTR and STZ myocytes (Supplementary material online, *Figure S10*), suggesting that SERCA2a down-regulation was not associated to changes in NCX activity in STZ myocytes. Treatment of STZ myocytes with istaroxime blunted differences between CTR and STZ.

Lastly, to estimate SR Ca^{2+} uptake function in the absence of NCX and NKA function, SR reloading protocol was applied in V-clamped cells by removing Na^+ from both sides of the sarcolemma as previously described.[21] As shown in *Figure 4C*, after SR depletion by caffeine superfusion, in comparison to CTR myocytes, the SR reloading process was slower in STZ myocytes, clearly confirming the SERCA2a down-regulation. In particular, in STZ myocytes, the rate of Ca_T increment was reduced and this was associated with a slower enhancement of the ER-gain. Moreover, the decay time constant, mostly representing SR Ca^{2+} uptake function, increased at each pulse, accordingly to a reduced SERCA2a function in STZ myocytes. Stimulation of SERCA2a by istaroxime caused faster SR reloading and all parameters were restored to CTR condition.

3.8 SERCA2a activity affects Ca^{2+} sparks characteristics

As shown before, both DADs and SCR events were detected only in few STZ myocytes, suggesting that SR stability is mostly preserved in this DCM model. To further analyse this point, Ca^{2+} sparks rate and characteristics were evaluated in all groups (*Figure 5*). Compared to CTR, STZ myocytes showed Ca^{2+} sparks with reduced amplitude, width, duration, and spark mass (*Figure 5B*), in agreement with a reduced SR Ca^{2+} content at resting. Istaroxime, by stimulating SERCA2a, partially restored Ca^{2+} sparks characteristics in STZ myocytes. In particular, istaroxime-induced SERCA2a stimulation emerged also by the analysis of Ca^{2+} sparks decay that significantly became faster in the presence of the compound. Sparks rate was not significantly affected by STZ and istaroxime.

4. Discussion

Aim of this study was to assess the effect of SERCA2a stimulation mediated by istaroxime in improving $Ca^{2+}{}_i$ dynamics in a diabetic rat model characterized by impaired diastolic function.

Several therapeutic approaches that increase SERCA2a function have been recently investigated.[18,40–43] However, despite of the intense research in discovering small molecules or gene therapy aimed at selectively activating SERCA2a, no promising clinical outcomes have been reached so far.

Istaroxime is the first-in-class original luso-inotropic agent targeting SERCA2a in addition to NKA inhibition, that has shown efficacy and safety in clinical trials on patients with acute HF syndrome.[20,28] In the past, *in vitro* istaroxime effects were largely characterized at concentrations showing dual mechanism of action.[21,23,27,29,30] In this study, lusitropic SERCA2a-dependent istaroxime effects were evaluated by testing istaroxime both *in vitro* and *in vivo* at concentrations marginally affecting NKA. Estimated drug plasma level at 15 min infusion and drug concentrations adopted for *in vitro* assays were largely comparable.

To our knowledge, no other small molecules active on SERCA2a at submicromolar concentration are available.

4.1 STZ-induced DCM. DD is associated to down-regulated SERCA2a expression and activity and is improved by istaroxime infusion

STZ rats showed a clear DD highlighted by changes in mitral inflow, in line with published results, reporting that DCM often manifests first as DD (*Table 2*). Our echo measurements evidenced marked alterations on DD indexes in STZ rats. In particular, we showed a significant transmitral Doppler flow enhancement of E wave DT and reduced E/A ratio in STZ rats. Analogously, TDI parameters, relatively unaffected by load, indicated a significant reduction of early diastolic myocardial velocity (e') and e'/a' with an increase of E/e' ratio in STZ rats. Systolic function appeared almost unaffected in STZ as compared to CTR rats, as indicated by FS and CO values. Moreover, we observed a marked

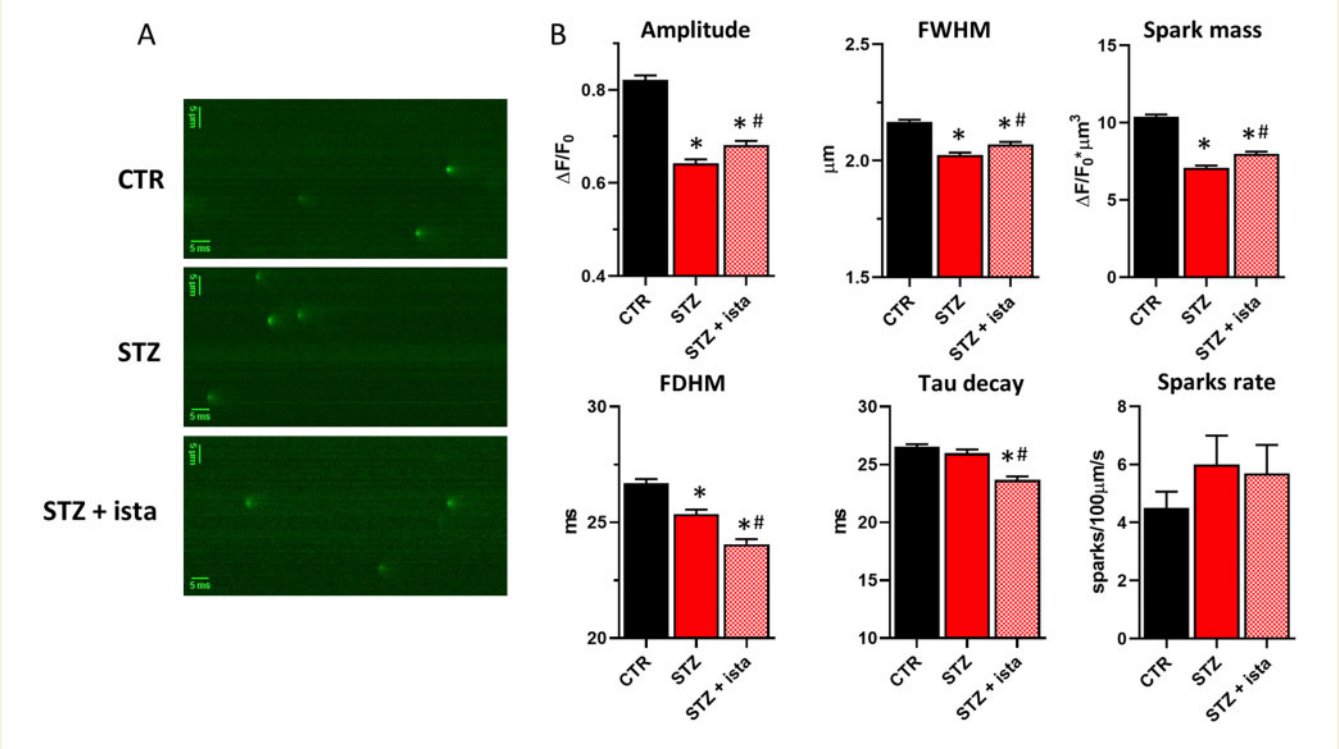

Figure 5 STZ-induced changes in Ca^{2+} sparks rate and characteristics. Analysis of istaroxime effects. (*A*) Representative xt images showing Ca^{2+} sparks at resting in CTR and STZ myocytes with or w/o 100 nmol/L istaroxime. (*B*) Statistics of Ca^{2+} sparks characteristics and rate for each group. *P<0.05 vs. CTR; #P<0.05 vs. STZ w/o istarpoxime (one-way ANOVA plus Tukey's multiple comparison); CTR N = 7 (n = 62, sparks # = 2789), STZ N = 5 (w/o istaroxime n = 53, sparks # = 2019, with istaroxime n = 47, sparks # = 1940). FWHM, full width at half maximum; FDHM, full duration at half maximum. Spark mass (spark amplitude*1.206* FWHM^3).

bradycardia, consistent with the impaired autonomic function and down-regulation of the expression of the pacemaker channel HCN4.[44]

Consistently with STZ-induced DD, in heart preparations and in cardiomyocytes from STZ rats, we observed a clear reduction of SERCA2 protein expression level, an increase of mPLN/SERCA2 ratio and a reduction of Ser^{16} phosphorylated mPLN (*Figure 1* and Supplementary material online, *Figure S7*). Conversely, CaMKII-dependent Thr^{17} phosphorylation of mPLN was similar between STZ and CTR rats (*Figure 1*). These biochemical alterations were associated with the reduction of SERCA2a ATPase activity observed in heart preparations from STZ compared to CTR rats (*Figure 1*) and indicate that these may translate into the impairment of diastolic function seen by the echocardiographic examination.

DCM is reported to be associated with cardiac fibrosis, which is responsible for increased LV stiffness and decreased ventricular wall compliance resulting in systolic and, in particular, DD.[45] However, in this study, no change of collagen type 1 and MMP-9 protein expression has been observed in LV from CTR and STZ rats, indicating that 8 weeks after STZ injection may be a time not long enough to develop this alteration. Moreover, several indexes indicated the absence of a concrete LV hypertrophy in STZ rats, because the increase in HW/BW was strictly dependent on BW loss. Otherwise, we observed reduced HW/TL and LV/HW ratios, results confirmed at the cellular level with reduced C_m, CSA, cell volume, and TT organization. These results are supported by a recent study showing reduced sinoatrial C_m in STZ-treated mice.[44] Loss of viable cardiomyocytes in STZ rats is also a possibility as previously shown.[46]

Collectively, these results indicate that STZ-induced DCM is characterized by impaired diastolic function associated with the down-regulation of SERCA2a expression and activity. This model is therefore suitable for testing the cardiac effects of SERCA2a stimulation by istaroxime. Istaroxime infused at 0.11 mg/kg/min for 15 min in STZ rats reverted the DD, inducing a significant reduction of DT and DT/E and an increase of e' (*Table 2*). The favourable mechanistic profile of istaroxime action is once again corroborated by our results in ameliorating DD in a DCM model.

4.2 STZ-induced changes in $Ca^{2+}{}_i$ dynamics and electrical activity. Istaroxime effects at a concentration marginally affecting NKA

Consequences of STZ-induced SERCA2a down-regulation were functionally analysed in isolated LV myocytes. In particular, the post-rest potentiation protocol clearly highlighted the reduced ability of SR to accumulate Ca^{2+} at resting in STZ myocytes in comparison to CTR ones. This resulted in Ca_D enhancement when pacing cells at 2 Hz (*Figure 2*); in spite of this, Ca_{SR} left unchanged, probably as a consequence of STZ-induced changes in electrical activity. Indeed, STZ induced marked APD prolongation at all stimulation rates (*Figure 3A*), according to voltage-dependent K^+ channels down-regulation.[37] Moreover, the lack of E_{diast} rate dependent hyperpolarization in STZ myocytes is in agreement with STZ-induced NKA down-regulation.[39]

AP-clamp experiments clearly demonstrated the relevance of AP waveform in controlling $Ca^{2+}{}_i$ dynamics (*Figure 4A*). Indeed, AP prolongation caused a sharp $Ca^{2+}{}_i$ loading. Thus, STZ-induced changes in electrical activity might indirectly affect $Ca^{2+}{}_i$ dynamics. In agreement with this, following the control of membrane potential (*Figure 4B*), direct effects of STZ-induced SERCA2a down-regulation were detected on $Ca^{2+}{}_i$ handling. In particular, by clamping myocytes at -35 mV, STZ induced Ca_{SR} and Ca_T amplitude reduction, effects that were unseen in intact field stimulated cells. Moreover, incubating myocytes in extracellular and intracellular $Na^+{}_i$ free solutions to remove NCX and NKA contribution (*Figure 4C*), SR Ca^{2+} uptake reloading kinetic following caffeine-induced SR depletion was clearly depressed in STZ myocytes.

Istaroxime stimulated SERCA2a in cardiac preparations from STZ rats by re-establishing the STZ-induced reduction of its maximal activity (V_{max}) without affecting its affinity for Ca^{2+} (K_d). Moreover, no effects on SERCA2a activity were detected in CTR heart preparation (*Figure 1*), indicating that the stimulatory action on SERCA2a is more remarkable when a pathological alteration (i.e. STZ-induced SERCA2a down-regulation) is present. Analogously, in dog cardiac SR vesicles, the stimulatory effect of istaroxime prevailed in the failing vs. healthy dog.[22] However, in healthy guinea pig cardiac microsomes, istaroxime stimulated SERCA2a by reducing the K_d Ca^{2+}.[21] The different effect of the compound on SERCA2a kinetic parameters in rat and dog (V_{max} enhancement) vs. guinea pig (K_d Ca^{2+} reduction) may not exclude species-specific differences in SERCA2a-PLN functional complex formation along the heart preparation, affecting istaroxime interaction. Furthermore, these kinetic changes across species might depend on how the compound interferes with species-specific SERCA2a-PLN complex domains. Although Ferrandi *et al.*[22] has already shown that istaroxime stimulates SERCA2a activity through a direct interaction with SERCA2a/PLN complex, favouring a partial dissociation of PLN from SERCA2a, further structural studies are still necessary to full understand istaroxime molecular mechanism of action.

At the cellular level, istaroxime stimulated SR Ca^{2+} uptake as clearly shown by applying the post-rest potentiation protocol to STZ myocytes (*Figure 2*). Moreover, as explain above, SERCA2a stimulation by the drug was fully remarkable by controlling membrane potential changes in voltage-clamped myocytes (*Figure 4*). Indeed, istaroxime, by stimulating SERCA2a, mostly restored STZ-induced changes in Ca_{SR} and Ca_T amplitude and it accelerated the SR uptake function, effects all compatible with a sharp enhancement of Ca^{2+} uptake by the SR, as expected from stimulation of SERCA2a activity.

STZ-induced Ca_D enhancement was blunted by istaroxime in paced STZ myocytes; by contrast, Ca_D was significantly increased by the drug in CTR myocytes. Moreover, istaroxime slightly depolarized E_{diast} in both CTR and STZ myocytes, as a result of a partial NKA blockade. Overall, the modulation of Ca_D by 100 nmol/L istaroxime might be the consequence of the balance between effects depending on SERCA2a stimulation and NKA inhibition, although negligible.

Abnormalities of the SR uptake function can be due to reduced SERCA2a activity or to increased Ca^{2+} leak through ryanodine receptor (RyR) channels. While functional and structural SERCA2a down-regulation (increased inhibition by PLN and reduced SERCA2a protein level) was observed, RyR open probability was not significantly changed in STZ myocytes. Indeed, Ca^{2+} sparks frequency (*Figure 5*), the incidence of Ca^{2+} waves and the related DADs were not significantly increased in STZ myocytes, thus suggesting the absence of a sharp SR instability at this stage of STZ-induced DCM. These findings lead to limit the detection of potential anti-arrhythmic effect of istaroxime as a direct consequence of SERCA2a stimulation.

Moreover, STZ-induced changes in Ca^{2+} sparks characteristics are a mirror image of the reduced SR Ca^{2+} content in STZ myocytes (*Figure 5*). Indeed, in comparison to CTR myocytes, Ca^{2+} sparks became smaller in amplitude, spatial and time duration, resulting in a smaller spark mass. Istaroxime, by stimulating SERCA2a, blunted these changes and even markedly accelerated Ca^{2+} sparks decay. The last event is

relevant for the potential anti-arrhythmic efficacy of istaroxime because of a faster Ca^{2+} release unit switch off, that can limit Ca^{2+} waves genesis. Moreover, the acceleration of Ca^{2+} spark decay induced by istaroxime seems independent on STZ-induced changes; thus, we cannot exclude direct effects of the drug on Ca^{2+} spark termination mechanisms.

Temporal dispersion of repolarization, quantified as STV of APD, is a well-known pro-arrhythmic index because plays an important role in the initiation of ventricular arrhythmias like *torsade de point*.[47] STV was significantly increased in STZ myocytes and this was mainly associated to APD prolongation (*Figure 3C*); istaroxime did not significantly affect STV.

4.3 Study limitation

The aim of the study was to test the effect of SERCA2a stimulation on DD in a DCM model. The study spreads from *in vivo* to *in vitro* effects of istaroxime at a concentration marginally affecting NKA. We would like to stress that even though effects dependent on NKA inhibition were detected, the general findings of the study are largely dependent on SERCA2a stimulation by the drug.

5. Conclusions and clinical implications

SERCA2a stimulation by istaroxime improves DD in diabetic rats, by controlling $Ca^{2+}{}_i$ compartmentalization. Thus, SERCA2a stimulation can be considered a promising therapeutic approach for DCM treatment. Even though the translation of drug effects from animal models to patients must take into account differences in the pathophysiological mechanisms/picture between animals and patients, STZ model was useful for studying the cardiac mechanical improvement produced by a drug endowed with a SERCA2a stimulatory activity. Accordingly, a recent phase II randomized clinical study in patients hospitalized for acute HF[28] showed that a 24 h infusion of istaroxime at 0.5 and 1 μg/kg/min improved cardiac function without major cardiac adverse effects. This is a proof-of-concept that SERCA2a stimulation is a novel and valid target for the treatment of high risk patients with reduced LVEF. Therefore, the development of small molecules active on SERCA2a only ('pure SERCA2a activators') might be clinically relevant to treat targeted patients with unfavourable cardiovascular outcomes with traditional therapies.

Supplementary material

Supplementary material is available at *Cardiovascular Research* online.

Authors' contributions

E.T. performed electrophysiological studies and drafted the manuscript; M.A. performed Ca^{2+} handling experiments; A.M.L. analysed data; E.S. and S.V. measured TT distribution and cell dimensions; M.F. and P.B. performed biochemical measurements; S.-C.H. and G.-J.C. performed *in vivo* measurements; E.B. and C.B. contributed to echocardiographic evaluations; C.A. analysed Ca^{2+} sparks; G.M. contributed with high-level technical assistance; P.F. and G.B. critically supervised the study; M.R. coordinated the study and wrote the manuscript.

Funding

This work was supported by CVie Therapeutics Limited (Taipei, Taiwan), Windtree Therapeutics (Warrington, USA), and FAR2019 of the University of Milano-Bicocca.

Conflict of interest: M.F. and P.B. are Windtree employees, P.F. and G.B. are Windtree consultants, S.-C.H. is employee of CVie Therapeutics Limited.

Data availability

The data underlying this article will be shared on reasonable request to the corresponding author.

References

1. Sherwin R, Jastreboff AM. Year in diabetes 2012: the diabetes tsunami. *J Clin Endocrinol Metab* 2012;**97**:4293–4301.
2. Schannwell CM, Schneppenheim M, Perings S, Plehn G, Strauer BE. Left ventricular diastolic dysfunction as an early manifestation of diabetic cardiomyopathy. *Cardiology* 2002;**98**:33–39.
3. Belke DD, Dillmann WH. Altered cardiac calcium handling in diabetes. *Curr Hypertens Rep* 2004;**6**:424–429.
4. Boudina S, Abel ED. Diabetic cardiomyopathy revisited. *Circulation* 2007;**115**:3213–3223.
5. Lebeche D, Davidoff AJ, Hajjar RJ. Interplay between impaired calcium regulation and insulin signaling abnormalities in diabetic cardiomyopathy. *Nat Clin Pract Cardiovasc Med* 2008;**5**:715–724.
6. Choi KM, Zhong Y, Hoit BD, Grupp IL, Hahn H, Dilly KW, Guatimosim S, Jonathan Lederer W, Matlib MA. Defective intracellular Ca^{2+} signaling contributes to cardiomyopathy in type 1 diabetic rats. *Am J Physiol Heart Circ Physiol* 2002;**283**:H1398–H1408.
7. Vasanji Z, Dhalla NS, Netticadan T. Increased inhibition of SERCA2 by phospholamban in the type I diabetic heart. *Mol Cell Biochem* 2004;**261**:245–249.
8. Kranias EG, Hajjar RJ. Modulation of cardiac contractility by the phopholamban/SERCA2a regulatome. *Circ Res* 2012;**110**:1646–1660.
9. Zaza A, Rocchetti M. Calcium store stability as an antiarrhythmic endpoint. *Curr Pharm Des* 2015;**21**:1053–1061.
10. Malek V, Gaikwad AB. Telmisartan and thiorphan combination treatment attenuates fibrosis and apoptosis in preventing diabetic cardiomyopathy. *Cardiovasc Res* 2019;**115**:373–384.
11. Dobrin JS, Lebeche D. Diabetic cardiomyopathy: signaling defects and therapeutic approaches. *Expert Rev Cardiovasc Ther* 2010;**8**:373–391.
12. Ng HH, Leo CH, Parry LJ, Ritchie RH. Relaxin as a therapeutic target for the cardiovascular complications of diabetes. *Front Pharmacol* 2018;**9**:501.
13. Jaski BE, Jessup ML, Mancini DM, Cappola TP, Pauly DF, Greenberg B, Borow K, Dittrich H, Zsebo KM, Hajjar RJ. Calcium upregulation by percutaneous administration of gene therapy in cardiac disease (CUPID Trial), a first-in-human phase 1/2 clinical trial. *J Card Fail* 2009;**15**:171–181.
14. Clark RJ, McDonough PM, Swanson E, Trost SU, Suzuki M, Fukuda M, Dillmann WH. Diabetes and the accompanying hyperglycemia impairs cardiomyocyte calcium cycling through increased nuclear O-GlcNAcylation. *J Biol Chem* 2003;**278**:44230–44237.
15. Shao CH, Capek HL, Patel KP, Wang M, Tang K, DeSouza C, Nagai R, Mayhan W, Periasamy M, Bidasee KR. Carbonylation contributes to SERCA2a activity loss and diastolic dysfunction in a rat model of type 1 diabetes. *Diabetes* 2011;**60**:947–959.
16. Kho C, Lee A, Jeong D, Oh JG, Gorski PA, Fish K, Sanchez R, Devita RJ, Christensen G, Dahl R, Hajjar RJ. Small-molecule activation of SERCA2a SUMOylation for the treatment of heart failure. *Nat Commun* 2015;**6**:7229.
17. Peng BY, Dubey NK, Mishra VK, Tsai FC, Dubey R, Deng WP, Wei HJ. Addressing stem cell therapeutic approaches in pathobiology of diabetes and its complications. *J Diabetes Res* 2018;**2018**:7806435.
18. Kaneko M, Yamamoto H, Sakai H, Kamada Y, Tanaka T, Fujiwara S, Yamamoto S, Takahagi H, Igawa H, Kasai S, Noda M, Inui M, Nishimoto T. A pyridone derivative activates SERCA2a by attenuating the inhibitory effect of phospholamban. *Eur J Pharmacol* 2017;**814**:1–8.
19. Bidasee KR, Zhang Y, Shao CH, Wang M, Patel KP, Dincer ÜD, Besch HR. Diabetes increases formation of advanced glycation end products on sarco(endo)plasmic reticulum Ca^{2+}-ATPase. *Diabetes* 2004;**53**:463–473.
20. Shah SJ, Blair JEA, Filippatos GS, MacArie C, Ruzyllo W, Korewicki J, Bubenek-Turconi SI, Ceracchi M, Bianchetti M, Carminati P, Kremastinos D, Grzybowski J, Valentini G, Sabbah HN, Gheorghiade M. Effects of istaroxime on diastolic stiffness in acute heart failure syndromes: results from the Hemodynamic, Echocardiographic, and Neurohormonal Effects of Istaroxime, a Novel Intravenous Inotropic and Lusitropic Agent: a Randomized Controlled Trial in Patients Hospitalized with Heart Failure (HORIZON-HF) trial. *Am Heart J* 2009;**157**:1035–1041.

21. Rocchetti M, Besana A, Mostacciuolo G, Micheletti R, Ferrari P, Sarkozi S, Szegedi C, Jona I, Zaza A. Modulation of sarcoplasmic reticulum function by Na+/K + pump inhibitors with different toxicity: digoxin and PST2744 [(E,Z)-3-((2-aminoethoxy)imino)androstane-6,17-dione hydrochloride]. *J Pharmacol Exp Ther* 2005;**313**:207–215.
22. Ferrandi M, Barassi P, Tadini-Buoninsegni F, Bartolommei G, Molinari I, Tripodi MG, Reina C, Moncelli MR, Bianchi G, Ferrari P. Istaroxime stimulates SERCA2a and accelerates calcium cycling in heart failure by relieving phospholamban inhibition. *Br J Pharmacol* 2013;**169**:1849–1861.
23. Alemanni M, Rocchetti M, Re D, Zaza A. Role and mechanism of subcellular Ca^{2+} distribution in the action of two inotropic agents with different toxicity. *J Mol Cell Cardiol* 2011;**50**:910–918.
24. Adamson PB, Vanoli E, Mattera GG, Germany R, Gagnol JP, Carminati P, Schwartz PJ. Hemodynamic effects of a new inotropic compound, PST-2744, in dogs with chronic ischemic heart failure. *J Cardiovasc Pharmacol* 2003;**42**:169–173.
25. Micheletti R, Palazzo F, Barassi P, Giacalone G, Ferrandi M, Schiavone A, Moro B, Parodi O, Ferrari P, Bianchi G. Istaroxime, a stimulator of sarcoplasmic reticulum calcium adenosine triphosphatase isoform 2a activity, as a novel therapeutic approach to heart failure. *Am J Cardiol* 2007;**99**:24A–32A.
26. Sabbah HN, Imai M, Cowart D, Amato A, Carminati P, Gheorghiade M. Hemodynamic properties of a new-generation positive luso-inotropic agent for the acute treatment of advanced heart failure. *Am J Cardiol* 2007;**99**:41A–46A.
27. Rocchetti M, Alemanni M, Mostacciuolo G, Barassi P, Altomare C, Chisci R, Micheletti R, Ferrari P, Zaza A. Modulation of sarcoplasmic reticulum function by PST2744 [Istaroxime; (E,Z)-3-((2-aminoethoxy)imino) androstane-6,17-dione hydrochloride] in a pressure-overload heart failure model. *J Pharmacol Exp Ther* 2008;**326**:957–965.
28. Carubelli V, Zhang Y, Metra M, Lombardi C, Felker GM, Filippatos G, O'Connor CM, Teerlink JR, Simmons P, Segal R, Malfatto G, La Rovere MT, Li D, Han X, Yuan Z, Yao Y, Li B, Lau LF, Bianchi G, Zhang J, Istaroxime ADHF Trial Group. Treatment with 24 hour istaroxime infusion in patients hospitalised for acute heart failure: a randomised, placebo-controlled trial. *Eur J Heart Fail* 2020;**22**:1684–1693.
29. Micheletti R, Mattera GG, Rocchetti M, Schiavone A, Loi MF, Zaza A, Gagnol RJP, De Munari S, Melloni P, Carminati P, Bianchi G, Ferrari P. Pharmacological profile of the novel inotropic agent (E,Z)-3-((2-aminoethoxy)imino)androstane-6,17-dione hydrochloride (PST2744). *J Pharmacol Exp Ther* 2002;**303**:592–600.
30. Rocchetti M, Besana A, Mostacciuolo G, Ferrari P, Micheletti R, Zaza A. Diverse toxicity associated with cardiac Na+/K+ pump inhibition: evaluation of electrophysiological mechanisms. *J Pharmacol Exp Ther* 2003;**305**:765–771.
31. Gheorghiade M, Ambrosy AP, Ferrandi M, Ferrari P. Combining SERCA2a activation and Na-K ATPase inhibition: a promising new approach to managing acute heart failure syndromes with low cardiac output. *Discov Med* 2011;**12**:141–151.
32. Bossu A, Kostense A, Beekman HDM, Houtman MJC, van der Heyden MAG, Vos MA. Istaroxime, a positive inotropic agent devoid of proarrhythmic properties in sensitive chronic atrioventricular block dogs. *Pharmacol Res* 2018;**133**:132–140.
33. Rocchetti M, Sala L, Rizzetto R, Irene Staszewsky L, Alemanni M, Zambelli V, Russo I, Barile L, Cornaghi L, Altomare C, Ronchi C, Mostacciuolo G, Lucchetti J, Gobbi M, Latini R, Zaza A. Ranolazine prevents INaL enhancement and blunts myocardial remodelling in a model of pulmonary hypertension. *Cardiovasc Res* 2014;**104**:37–48.
34. Pasqualin C, Gannier F, Malécot CO, Bredeloux P, Maupoil V. Automatic quantitative analysis of t-tubule organization in cardiac myocytes using ImageJ. *Am J Physiol Cell Physiol* 2015;**308**:C237–C245.
35. Ferrandi M, Tripodi G, Salardi S, Florio M, Modica R, Barassi P, Parenti P, Shainskaya A, Karlish S, Bianchi G, Ferrari P. Renal Na,K-ATPase in genetic hypertension. *Hypertension* 1996;**28**:1018–1025.
36. Altomare C, Bartolucci C, Sala L, Bernardi J, Mostacciuolo G, Rocchetti M, Severi S, Zaza A. IKr impact on repolarization and its variability assessed by dynamic clamp. *Circ Arrhythm Electrophysiol* 2015;**8**:1265–1275.
37. Meo M, Meste O, Signore S, Sorrentino A, Cannata A, Zhou Y, Matsuda A, Luciani M, Kannappan R, Goichberg P, Leri A, Anversa P, Rota M. Reduction in Kv current enhances the temporal dispersion of the action potential in diabetic myocytes: insights from a novel repolarization algorithm. *J Am Heart Assoc* 2016;**5**:e003078.
38. Howarth FC, Jacobson M, Qureshi MA, Shafiullah M, Hameed RS, Zilahi E, Al Haj A, Nowotny N, Adeghate E. Altered gene expression may underlie prolonged duration of the QT interval and ventricular action potential in streptozotocin-induced diabetic rat heart. *Mol Cell Biochem* 2009;**328**:57–65.
39. Ku DD, Sellers BM. Effects of streptozotocin diabetes and insulin treatment on myocardial sodium pump and contractility of the rat heart. *J Pharmacol Exp Ther* 1982;**222**:395–400.
40. Hoshijima M, Ikeda Y, Iwanaga Y, Minamisawa S, Date MO, Gu Y, Iwatate M, Li M, Wang L, Wilson JM, Wang Y, Ross J, Chien KR. Chronic suppression of heart-failure progression by a pseudophosphorylated mutant of phospholamban via in vivo cardiac rAAV gene delivery. *Nat Med* 2002;**8**:864–871.
41. Suckau L, Fechner H, Chemaly E, Krohn S, Hadri L, Kockskamper J, Westermann D, Bisping E, Ly H, Wang X, Kawase Y, Chen J, Liang L, Sipo I, Vetter R, Weger S, Kurreck J, Erdmann V, Tschope C, Pieske B, Lebeche D, Schultheiss HP, Hajjar RJ, Poller WC. Long-term cardiac-targeted RNA interference for the treatment of heart failure restores cardiac function and reduces pathological hypertrophy. *Circulation* 2009;**119**:1241–1252.
42. Watanabe A, Arai M, Yamazaki M, Koitabashi N, Wuytack F, Kurabayashi M. Phospholamban ablation by RNA interference increases Ca^{2+}uptake into rat cardiac myocyte sarcoplasmic reticulum. *J Mol Cell Cardiol* 2004;**37**:691–698.
43. Suzuki T, Wang JH. Stimulation of bovine cardiac sarcoplasmic reticulum Ca^{2+} pump and blocking of phospholamban phosphorylation and dephosphorylation by a phospholamban monoclonal antibody. *J Biol Chem* 1986;**261**:7018–7023.
44. Zhang Y, Wang Y, Yanni J, Qureshi MA, Logantha SJRJ, Kassab S, Boyett MR, Gardiner NJ, Sun H, Howarth FC, Dobrzynski H. Electrical conduction system remodeling in streptozotocin-induced diabetes mellitus rat heart. *Front Physiol* 2019;**10**:1–15.
45. Mihm MJ, Seifert JL, Coyle CM, Bauer JA. Diabetes related cardiomyopathy time dependent echocardiographic evaluation in an experimental rat model. *Life Sci* 2001;**69**:527–542.
46. Wu W, Liu X, Han L. Apoptosis of cardiomyocytes in diabetic cardiomyopathy involves overexpression of glycogen synthase kinase-3β. *Biosci Rep* 2019;**39**:BSR20171307.
47. Smoczynska A, Beekman HDM, Vos MA. The increment of short-term variability of repolarisation determines the severity of the imminent arrhythmic outcome. *Arrhythm Electrophysiol Rev* 2019;**8**:166–172.

Translational perspective

Deficient SR Ca^{2+} uptake has been identified in cardiomyocytes from failing human hearts with impaired diastolic relaxation (e.g. diabetic hearts) and has been associated with a decreased SERCA2a expression and activity and/or with a higher SERCA2a inhibition by PLN. Thus, SERCA2a may represent a pharmacological target for interventions aimed at improving cytosolic Ca^{2+} compartmentalization into the SR to limit diastolic dysfunction pathologies. In this context, istaroxime is the first-in-class luso-inotropic agent targeting SERCA2a that has already demonstrated its efficacy in clinical trials and may be useful to clarify the relevance of SERCA2a stimulation in controlling cytosolic Ca^{2+} level.